Universal linear relations between susceptibility and T_c in cuprates

Amit Kanigel, Amit Keren, Arkady Knizhnik, and Oren Shafir
Department of Physics, Technion-Israel Institute of Technology, Haifa 32000, Israel
(Received 18 October 2004; revised manuscript received 18 February 2005; published 29 June 2005)

We develop an experimental method for measuring the intrinsic susceptibility χ of the powder of cuprate superconductors in the zero-field limit using a dc magnetometer. The method is tested with lead spheres. Using this method, we determine χ for a number of cuprate families as a function of doping. A universal linear (and not proportionality) relation between T_c and χ is found. We suggest possible explanations for this phenomenon.

DOI: 10.1103/PhysRevB.71.224511 PACS number(s): 74.72.−h, 63.20.Mt, 64.70.Dv, 75.30.Cr

I. INTRODUCTION

Among the basic properties of a superconductor is its ability to expel a magnetic field, i.e., the Meissner effect. In all the metallic superconductors, the diamagnetic effect is complete, and below T_c, the susceptibility χ equals −1. In the high-temperature superconductors (HTSC) of the cuprates, the situation is far from being so simple, and there is growing evidence of samples showing an incomplete Meissner effect and even a paramagnetic Meissner effect.[1] At the same time, there has been an accumulation of results showing that the superconducting ground state in these materials is inhomogeneous.[2] Therefore, it is possible that the partial Meissner effect ($\chi<-1$) in the cuprates is an intrinsic property. This possibility motivated us to perform a comprehensive study of dc susceptibility in cuprates. We look for correlations between T_c and χ in different HTSC families and various doping.

It is important to mention that Panagopoulos *et al.* measured the ac susceptibility of $La_{2-y}Sr_yCuO_4$ and $HgBa_2CuO_{4+\delta}$ families.[3] However, they were not interested in comparing the absolute value of χ between the families and concentrated only on comparing the temperature dependence of the penetration depth between χ and μSR measurements, which resulted in very good agreement.

The difficulty of determining the absolute value of χ is caused by the granular nature of the cuprates and their ability to pin flux very easily. Consequently, the magnetization in these samples depends very much on the measurement procedure. For example, cooling a sample in a field, or cooling in zero field and then applying the field, will result in a different magnetization. On the other hand, the intrinsic susceptibility of a sample must be well defined and one should be able to compare different samples.

Therefore, we first develop the condition under which the measurements lead to the intrinsic susceptibility of the cuprates. The development of these conditions is based on experience gained while trying to measure the magnetization of a bundle of lead spheres. Second, we look for correlation between T_c and χ in different HTSC families with various doping. Our major finding is a universal linear relation between T_c and χ.

Our χ measurements are done on a set of HTSC families, which are different in many senses. The different families are $La_{2-y}Sr_yCuO_4$ (LSCO), $YBa_2Cu_3O_y$ (YBCO), and its less known "cousin" $(Ca_xLa_{1-x})(Ba_{1.75-x}La_{0.25+x})Cu_3O_y$ (CLBLCO) system with four different values of x. The CLBLCO[4] system in particular is ideal for our study due to several interesting properties. Each value of x generates the full superconductivity dome from the underdoped to the overdoped, and the maximum T_c is x-dependent. Thus, each x can be considered as a superconducting family. For all values of x and y CLBLCO is tetragonal, so there are no structural transformations that can cause a change in the volume of the unit cell.

II. SAMPLE PREPARATION

Ceramic samples of LSCO, YBCO, and CLBLCO were made by solid-state reaction. For LSCO, stoichiometric amounts of La_2O_3, $SrCO_3$, and CuO were mixed and ground using a ball mill. The mixtures were fired in air for 1–2 days; this was repeated three times. After pelleting, the samples were sintered in O_2 for about 64 h. The sintering temperature varied between 1100 and 1175 °C, depending on the Sr level; then the samples were cooled to room temperature at a rate of 10°/h.

For YBCO, the starting materials were Y_2O_3, $BaCO_3$, and CuO. The mixture was fired in air at 910 °C, then pelletized and fired again at 930 °C; the last step was then repeated. We also prepared pellets using YBCO that was supplied by PRAXAIR. This sample is made by combustion spray pyrolysis; the grains' average size is 3.9 μm. The pellets of the two kinds of YBCO were then sintered in O_2 for 60 h at 970 °C and cooled at a rate of 10°/h down to 510 °C and at a rate of 5°/h to 410 °C. The samples were kept at 410 °C for 5 days and then cooled down to room temperature at a rate of 10°/h.

The results presented in this paper for YBCO are from the two types of samples. No difference can be detected, meaning that the results are not sensitive to the preparation method of the samples.

The sample oxygen level, y, was then reduced by baking the sample in O_2 and quenching the samples in liquid nitrogen. For very underdoped samples, the reduction was done in a nitrogen atmosphere. The reduction temperatures are listed in Table I. The preparation of the CLBLCO samples is described elsewhere.[4]

The oxygen level of all the samples was determined by iodometric titration. In the LSCO samples, the deviation of the oxygen level from 4 is less than 0.005.

TABLE I. Summary of all the YBCO samples and the parameter values used in their preparation. T_r is the reduction temperature.

T_c (K)	y	T_r (°C)	Atmosphere	Material
92(1)	6.983			PRAXAIR
86.7(2)	6.855	530	O_2	Technion
56.7(2)	6.549	740	O_2	Technion
50.5(2)	6.489	810	O_2	Technion
40(2)	6.399	840	O_2	PRAXAIR
20(2)	6.3	580	N_2	PRAXAIR

The T_c of all the samples is determined using resistivity measurements. In order to compare all the samples, and to overcome the nontrivial problem of the relation between the chemical doping and p, we plot in Fig. 1 a unified phase diagram using the Presland *et al.* formula[5]

$$T_c/T_{c,\max} = 1 - 82.6(p - 0.16)^2 \tag{1}$$

which relates T_c and the hole density p.

Scanning electron microscopy (SEM) pictures show that the grain sizes in our YBCO and CLBLCO for different values of x, are of the same order of magnitude, and that the grains are agglomerates of crystalline whose typical length is $l \sim 1-10$ μm. An example can be seen in Fig. 2. These properties ensure that the demagnetization factor is similar for the different families.

III. EXPERIMENTAL METHOD

The susceptibility measurements were done using a home-built magnetometer based on a primary coil, two compensating secondary coils, and an extraction motor. Some results were verified with QD-SQUID at Bar-Ilan University and with a Cryogenic S600 SQUID magnetometer recently installed in our lab. The measurements were done in field-cooled conditions (FC), namely, for field changes the sample was warmed above T_c and cooled down in the new field. Since we use a superconducting magnet, there is always trapped flux in the magnet leading to a constant shift in the field values. For that reason, the magnetization is measured over a range of positive and negative fields. The susceptibility is defined by

$$\chi = \lim_{H\to 0} \frac{1}{V}\frac{dm}{dH}, \tag{2}$$

where m is the magnetization obtained from the induced signal at the secondary coils, H is the external field, and V is obtained from mass/density. The calibration of the magnetometer is explained below. The definition of V requires clarification. The problem in powder samples is to achieve conditions where the volume out of which the field is expelled, V_{sc}, equals V. The zero-field-cooling condition (ZFC) could result in a shielding volume V_{sc} which is bigger than V because in certain geometries Josephson connections can lead to shielding currents enclosing nonsuperconducting regions in the sample. The field-cooled conditions, on the other hand, lead to the Meissner volume and could result in a V_{sc} which is smaller than V due to flux pinning. Therefore, our first challenge is to find the appropriate measurement conditions, where V obtained from mass/density is exactly the volume out of which the field is expelled for powders.

In order to gain experience, we performed a preliminary experiment with Pb spheres where the theoretical χ is well known since Pb is a type I superconductor, so λ is negligible. We used a sphere diameter of 0.5 mm, and assumed that χ is the susceptibility of a single sphere including the demagnetization factor $(-3/2)$ and obtained $V_{sc} = \lim_{H\to 0}(1/\chi)(dm/dH)$. We calibrated the susceptometer using a few spheres mixed with sand so that they were very well separated from each other. Raw data are presented in the inset of Fig. 3, where we show curves of $M=m/V$ versus H for three samples: (i) the few Pb spheres mixed with sand (17.24 mg); (ii) a layer of Pb spheres (55.81 mg); and (iii) a

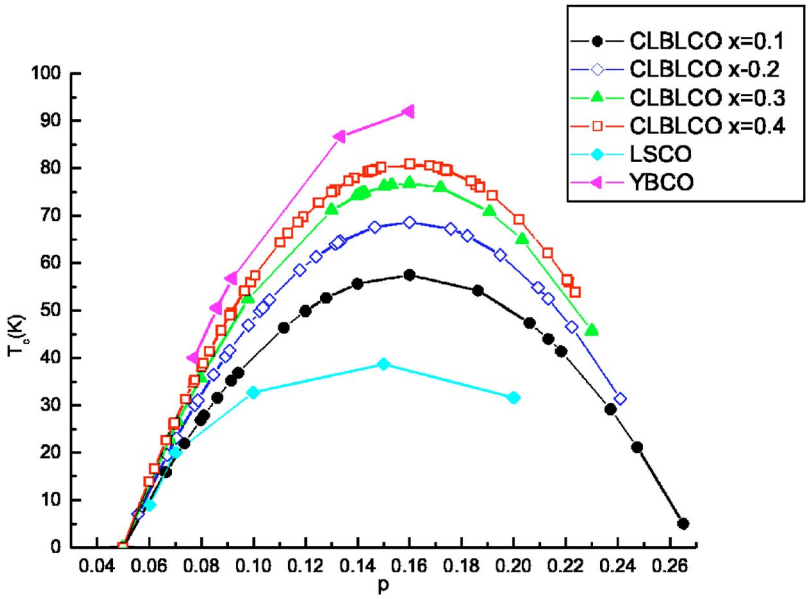

FIG. 1. (Color online) The phase diagram of CLBLCO, LSCO, and YBCO after conversion of chemical doping to hole doping p using Eq. (1).

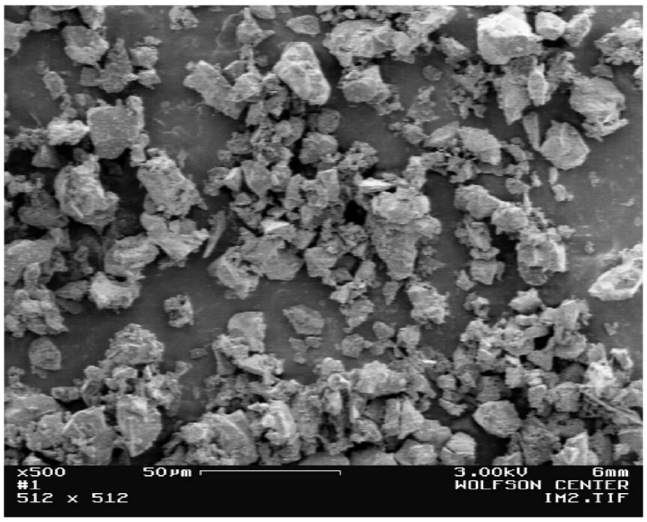

FIG. 2. SEM picture of a CLBLCO sample with $x=0.4$ and $y=6.983$.

full container of Pb spheres (634.5 mg). In all cases, a linear field dependence is observed at low fields. In the first and third cases, we find the same slope at $H\rightarrow 0$, but both are different from the second case. This means that isolated spheres and a full container of spheres give the same result.

Our findings in terms of $f=V_{sc}/V$ are summarized in Fig. 3, where f is depicted as a function of sample mass, and as a function of height of spheres in the container (h) over its diameter (d), on the lower and upper abscissa, respectively. For a small number of Pb spheres, which form a 2D layer at the bottom of the container ($h/d<1$), we find $f>1$. As the number of spheres increases, the volume they occupy in the

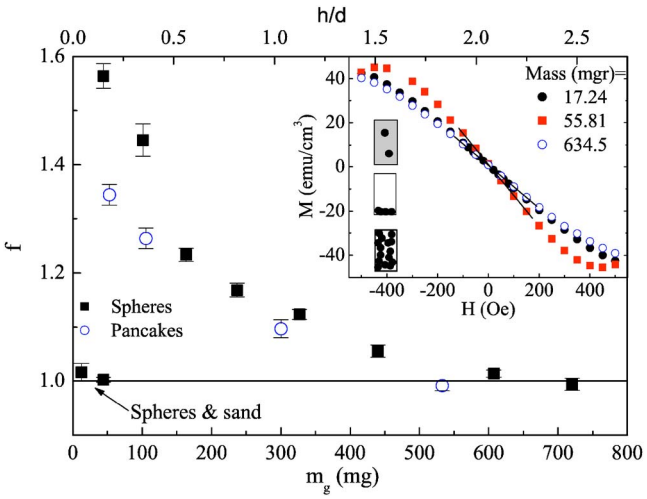

FIG. 3. (Color online) The volume fraction f of lead, which is the superconducting volume obtained from χ measurements, divided by the real volume taken from mass/density, plotted vs the mass of samples. In the top axis, we show also the dimensionality of the powder as the height it occupies in the sample container divided by its diameter. The solid squares represent sphere-shaped grains and open circles represent pancake-shaped grains. In the inset, we show the magnetization curves for three characteristic cases described in the text.

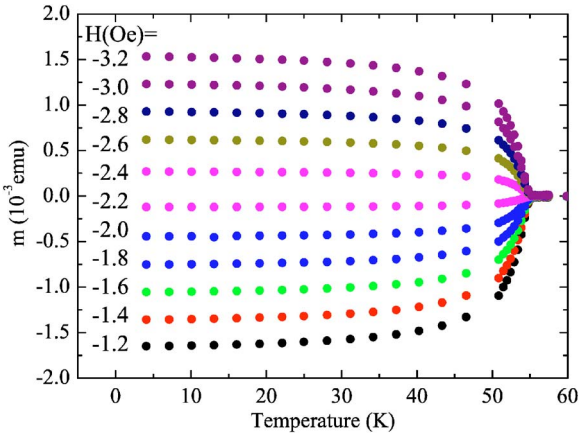

FIG. 4. (Color online) Field-cooled magnetization vs temperature in a variety of fields, in the small field limit where $H\ll\Phi_0/d^2$ and d is typical grain size.

container becomes 3D in nature ($h/d>1$), and f converges to 1. We repeated the experiment with "pancake"-shaped pieces of lead; the results are qualitatively the same. This leads to one of the important findings of this work. As long as FC conditions prevail and we use large values of h/d, we can safely assume that $V_{sc}=V$. This means that the magnetic field wanders inside the sample, in between the different grains, and fills all the empty spaces.

In the cuprates, χ of course is unknown, yet it is possible to check if the experimental conditions developed for Pb apply here as well. For this we determined the magnetization m in an FC procedure for various applied fields. We used fields which are small enough that even one flux quanta $\Phi_0=20$ Oe μm^2 cannot penetrate our grains (cross-section scale $A\sim 1$ μm^2), namely, $H\ll\Phi_0/A=20$ Oe. One such measurement is shown in Fig. 4. Only data in the sub-Oe fields is presented. The magnetization at the lowest temperature as a function of field is then plotted in Fig. 5. In this figure, a single line seems to fit the entire field range. However, when zooming in on the sub-Oe region, which is shown in the inset, a global shift of the line with respect to the fit is seen between negative and positive fields (due to bias currents in the power supply). Therefore, we fit m versus H to two different lines in a 10 Oe field range around zero magnetization, and obtain the susceptibility only from the averaged slope according to Eq. (2). However, outside this 20 Oe field range, a kink in the magnetization appears which we believe indicates the first vortex that enters into a grain. Therefore, all data in our experiment were acquired using this 20 Oe field range in steps of 1 Oe. We are aware of works showing a significant nonlinear field dependence of the magnetization in single crystals, especially in very low fields (mOe).[6,7] However, we did not see any deviation from linearity in our experimental conditions over this 20 Oe range.

To demonstrate that it is the intrinsic susceptibility of the cuprates that we are measuring, we present four tests. First, we performed the susceptibility measurements as a function of mass for a CLBLCO sample with $T_c=42.3$ K in a cylindrical sample holder of 5 mm inner diameter. Again, large mass means a 3D cylindric-like sample. In contrast, the sample resembles a disk when the mass is small. As can be

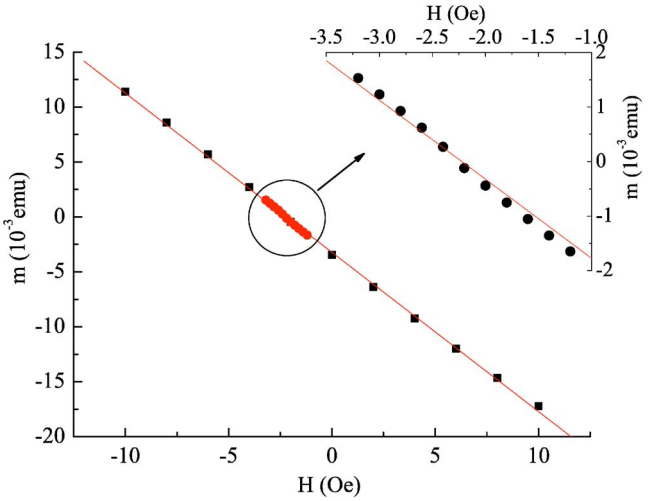

FIG. 5. (Color online) The zero-temperature magnetization after field cooling is plotted as a function of applied field. The field scale is shifted due to flux trapped in the superconducting magnet. Nevertheless, a straight line seems to fit the data well. Only a zoom in the zero magnetization region, depicted in the inset, shows that the shift is not identical on the two sides of zero magnetization. The susceptibility is determined by fitting the data to two lines, on different sides of zero magnetization, and taking the averaged slope.

seen in Fig. 6, χ decreases with increasing mass and saturates. All our measurements are therefore done with large mass. Second, we use a set of sieves, and divide the powder grains into two groups: 20 μm$<d<$40 μm and $d<$20 μm, where d is the characteristic size of a grain. We measured χ of these two samples both in FC and ZFC conditions, and the results are shown in Figs. 7(a) and 7(b), respectively. There is hardly any grain size dependence in the FC measurements, especially when compared to the ZFC experiment. This indicates that the grain size does not play a role in determining χ as long as we use the FC procedure.

Third, due to the combination of weak flux pinning (compared to low-T_c superconductors) and high temperatures, the time dependence of the magnetization can be very complex. Our main interest here is to find the optimal cooling scheme

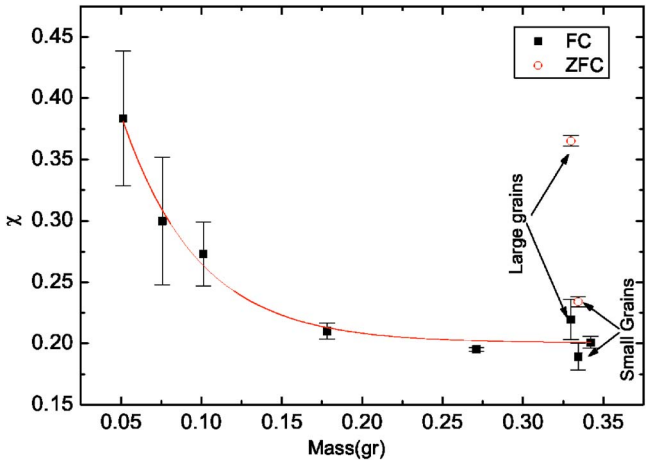

FIG. 6. (Color online) χ vs mass for a CLBLCO sample with T_c=42.3 K.

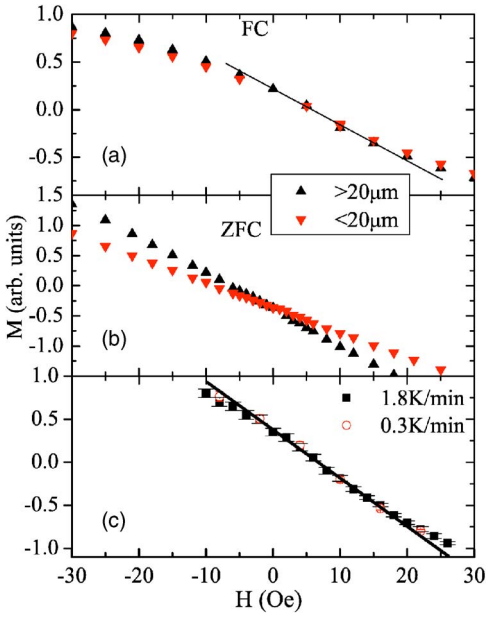

FIG. 7. (Color online) The magnetization curves for two grain sizes both in (a) FC and (b) ZFC. (c) depicts measurements for two different cooling rates.

in a field in order to obtain reproducible magnetization at base temperatures. We checked the susceptibility of a sample as a function of the cooling rate. We found, in agreement with previous works,[8] that in FC conditions it is important to pass through T_c slowly. Therefore, in all our measurements we cool the samples slowly enough so that no difference in the measurements is observed by cooling them even more slowly. This is demonstrated in Fig. 7(c), where we show that cooling at two different rates does not vary our result.

As a final test, we measured the magnetization of a $T_c\sim$40 K LSCO sample, first in the form of a sintered pellet and then of the powder after pulverization. The results are shown in Fig. 8. In the ZFC measurements, there is a great difference between the magnetization of the pellet and of the powder. While for the powder we observed the linear behavior we saw before, for the pellet we find a more complex

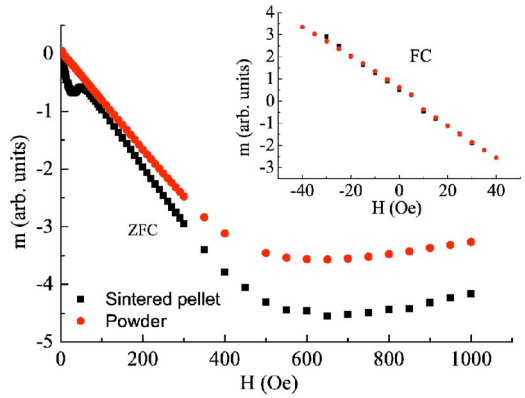

FIG. 8. (Color online) Magnetization measurements in FC and ZFC conditions of a sintered pellet and powder obtained by pulverizing the pellet. In FC conditions, there is no difference between the two samples.

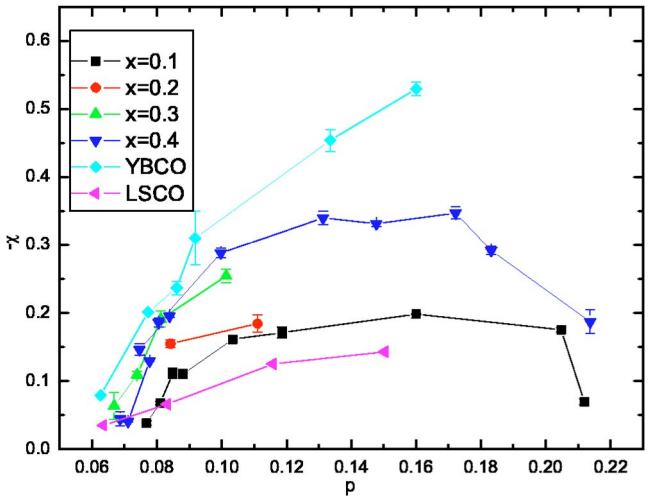

FIG. 9. (Color online) The negative susceptibility as a function of hole doping p taken from Eq. (1).

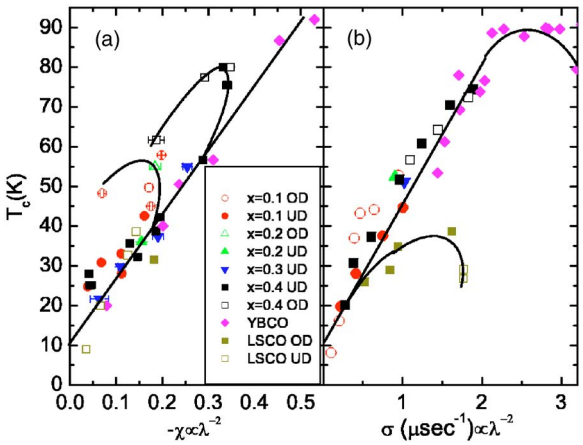

FIG. 10. (Color online) (a) T_c vs $-\chi$ at $T=1.6$ K for various samples of CLBLCO, YBCO, and LSCO. (b) T_c vs the muon depolarization rate σ at $T=1.8$ K for the same CLBLCO samples. Data for YBCO and LSCO are from Ref. 14.

curve. Up to 20 G, the calculated susceptibility is almost -1, indicating a shielding supercurrent that keeps the entire volume of the sample free of magnetic flux. Above this field, the susceptibility decreases and reaches a value similar to that of the powder. The difference between the two samples is only the connection between the grains. Those can be described as Josephson junctions with some average critical field, H_{Jc1}. Above this field, the intergrain links cannot support the shielding current, and flux penetrates into the space between the grains and we get local shielding of the grains as in the powder.

On the other hand, the FC measurements give a different picture. The magnetization is linear in all fields, both for the pellet and for the powder. Furthermore, the susceptibility is identical for both samples. This indicates that the intergrain links cannot support any Meissner currents at all. The field is not expelled from the volume in between grains even at fields below H_{Jc1}.

The different behavior of the FC and ZFC measurements in the pellet sample demonstrates another advantage of our measurement procedure: it is not sensitive to the connectivity between grains.

We interpret the results of all the above tests as reaching experimental conditions where small variations of these conditions have no affect on χ. Therefore, we believe that our experiments are in the limit where χ is the intrinsic susceptibility of the cuprates.

IV. RESULTS

In Fig. 9, we show the FC susceptibility of all our samples as a function of p, the hole concentration, where p is calculated using Eq. (1). The curves of $-\chi$ versus p resemble the phase diagram of Fig. 1, leaving no doubt that T_c and χ are somehow related.

In Fig. 10(a), we present T_c versus $-\chi$ for all samples. We find that T_c increases linearly (at low doping) with increasing $-\chi$, and the linear relation is identical for all families (within experimental errors). This is the main and theory-independent finding of this work. It is important to mention that no correlation between χ and T_c was found when the measurements were done in ZFC conditions.

V. DISCUSSION

The fact that all the samples obey the same linear relation between T_c and χ is very surprising, given the differences between these cuprate families. It may be that, because of the complexity of these materials, a new effective media theory is needed to explain this relation. Nevertheless, we would like to offer a simpler explanation for our data based on two experimental observations. On the one hand, it is well known that in the cuprates there is a universal linear relation between T_c and the inverse in-plane penetration depth squared,[9] known as the Uemura relation. This relation was revealed by a comprehensive comparison of the penetration depth, measured by the muon spin relaxation (μSR) technique, between different families of HTSC. On the other hand, based on the growing evidence for inhomogeneity in the cuprates and our observation that χ is independent of grain size and connectivity (see Figs. 7 and 8), it is conceivable that the length scale of grain sizes observed in Fig. 2 is not the correct grain size. Therefore, we speculate that the agglomerates seen in Fig. 2 are made of a very large number of even smaller units stuck together, and that their number is so large that the size of each one is smaller than the penetration length, at least in the low doping regime. In this approach, the true effective grain size length scale a would be a parameter to be determined experimentally.

In type II superconductors such as the HTSC, the penetration length plays an important role in the susceptibility, and $\chi=-b[1-g(x)/x]$,[10,11] where $x=a/\lambda$. In spherical, plane, and cylindrical shaped grains, $b=3/2$, 1, 1, and $g(x)$ is the Langevin, hyperbolic tangent, and the modified Bessel functions, respectively.[10,11] Under the assumed long penetration length assumption ($a/\lambda<1$), $g(x)/x$ can be expanded to give $\chi=-ca^2\lambda^{-2}$ with $c=1/10, 1/3$, and $1/4$ for the spherical,

plane, and cylindrical shaped cases, respectively. We further speculate that $\chi(\lambda)=O(\lambda^{-2})$ for all geometries. The anisotropy of the cuprates results in the replacement $\lambda=1.3\lambda_{ab}$.[12] After averaging over all grain shapes and sizes, we expect

$$\chi=-\bar{c}\frac{a^2}{\lambda_{ab}^2}, \tag{3}$$

where $\bar{c}$ is the averaged c and is a number on the order of unity (including the factor 1.3).

We also performed μSR measurements on sintered pellets made from the same CLBLCO powders, at the Paul Scherrer Institute (PSI) Switzerland, by field cooling in 3 kOe to 1.8 K. A full account of these measurements in CLBLCO is given in Ref. 13, and the YBCO and LSCO data were taken from Ref. 14. Figure 10(b) depicts T_c versus σ for all the samples. Here we used T_c from μSR as in the original Uemura plot.

A comparison between the two plots reveals interesting information. First, by comparing the μSR and susceptibility results, we can estimate a. For this we fit both T_c versus σ and χ in the underdoped region to straight lines with offsets σ_0 and χ_0. The solid lines in Figs. 10(a) and 10(b) are given by

$$T_c=-K_\chi(\chi+\chi_0) \tag{4}$$

and

$$T_c=K_\mu(\sigma+\sigma_0), \tag{5}$$

respectively, where $K_\mu=62(5)\mathrm{K}\,\mu\mathrm{s}$ and where $K_\chi=145(5)$ K. We determine a by making $K_\mu\sigma$ and $-K_\chi\chi$ agree with each other once they are expressed in terms of λ_{ab}. Taking $\sigma=7\times10^6\,\lambda_{ab}^{-2}$,[15] where σ is in μs^{-1} and λ_{ab} in angstroms, and χ from Eq. (4), we obtain

$$7\times10^6K_\mu\lambda_{ab}^{-2}=K_\chi\bar{c}a^2\lambda_{ab}{}^{-2}. \tag{6}$$

Solving this equation with $\bar{c}\lesssim1$, we find $a\gtrsim200$ nm. This length scale, which is smaller than the typical crystalline size estimated from SEM, could be due to defects or an intrinsic separation into domains. The same length scale was also found independently by ac susceptibility in YBCO and was ascribed to twinning.[16] However, our experiment shows that this is not the origin of a since CLBLCO and LSCO have no twinning.

Second, there is an offset in both χ and σ so that at $\lambda_{ab}\to\infty$ we find $T_c\sim10$ K. This universal deviation from strict proportionality between T_c and λ^{-2} is in agreement with the measurements of Zuev *et al.* on YBCO films.[17] The susceptibility offset could be explained by free spin that is present in underdoped HTSC and freeze as a spin glass.[18] The expected susceptibility of paramagnetic spins is given by $\chi=4\pi N\mu_{\mathrm{eff}}^2/(3k_BTV)$, where the 4π is introduced here since we normalized the susceptibility in Fig. 10 so that $\chi=-1$ for a superconductor [instead of $-1/(4\pi)$]. Taking $\mu_{\mathrm{eff}}=1.9\mu_B$ per Cu, $T=1.6$ K , $N=3$ spins in a unit cell, and V the volume of a cell, we find $\chi^0\sim0.1$. However, free spin cannot explain the offset in the μSR σ since they tend to increase σ rather than decrease it, namely, with spins σ is never zero. A different explanation for the offset, suggested in Ref. 17 , is that $T_c\propto\lambda_{ab}^{-2p}$ with $p\sim1/2$. This power law is most pronounced in the region $T_c<10$ K. This region is beyond the scope of our measurements, but $p\sim1/2$ at ultralow doping will give an artificial offset of the T_c versus $-\chi$ or σ for "normal doping" ($T_c>10$).

Third, panel (b) shows the well known boomerang effect in YBCO and LSCO, namely, overdoped samples have higher σ than underdoped ones with the same T_c. In CLBLCO there is an antiboomerang in both μSR and χ measurements, especially for the $x=0.1$ sample. This is a surprising result since it means that in overdoped CLBLCO, where the hole concentration is large, there is in fact a smaller superfluid density ($n_s\propto\lambda_{ab}^{-2}$) than in underdoped samples with smaller hole concentration.

VI. CONCLUSIONS

We found a universal linear dependence for underdoped HTSC between T_c and χ for different families, with doping as an implicit parameter. A possible explanation for this dependence is that in underdoped compounds the penetration depth λ_{ab} is longer than an effective grain size length scale a, which is much smaller than the grain size measured using SEM. In that case χ is proportional to $a^2\lambda_{ab}^{-2}$. By comparing $T_c(\chi)$ and $T_c(\sigma)$, we estimate $a\gtrsim200$ nm. The amazing aspect of this new grain size is that it is independent of sample preparation, type of compound, and doping. It appears to be similar to domain size in ferromagnets which are not determined by the sample size. In addition, our universal line does not cross the origin in the T_c, χ plane indicating universal deviation from strict proportionality between T_c and λ^{-2}.

ACKNOWLEDGMENTS

We would like to thank the PSI facility for their kind hospitality and continuing support of this project. We are grateful to Y. Yeshurun for the use of his QD-SQUID magnetometer and for very helpful discussions. This work was funded by the Israeli Science Foundation and the Posnansky Research Fund in High Temperature superconductivity. A. Kanigel acknowledges support from the Lady Davis fellowship.

[1] P. Svedlindh, K. Niskanen, P. Norling, P. Nordblad, L. Lundgren, B. Lonnberg, and T. Lundstrom, Physica C **162-164**, 1365 (1989); W. Braunisch, N. Knauf, V. Kataev, S. Neuhausen, A. Grutz, A. Kock, B. Roden, D. Khomskii, and D. Wohlleben, Phys. Rev. Lett. **68**, 1908 (1992).

[2] K. M. Lang, V. Madhavan, J. E. Hoffman, E. W. Hudson, H. Eisaki, S. Uchida, and J. C. Davis, Nature (London) **415**, 412 (2002).

[3] C. Panagopoulos, B. D. Rainford, J. R. Cooper, W. Lo, J. L. Tallon, J. W. Loram, J. Betouras, Y. S. Wang, and C. W. Chu, Phys. Rev. B **60**, 14 617 (1999).
[4] D. Goldschmidt, G. M. Reisner, Y. Direktovitch, A. Knizhnik, E. Gartstein, G. Kimmel, and Y. Eckstein, Phys. Rev. B **48**, 532 (1993).
[5] M. R. Presland, J. L. Tallon, R. G. Buckley, R. S. Liu, and N. E. Flower, Physica C **176**, 95 (1991).
[6] L. Krusin-Elbaum, A. P. Malozemoff, and Y. Yeshurun, in *High Temperature Superconductors*, edited by M. B. Brodsky, R. C. Dynes, K. Kitazawa, and H. L. Tuller (Material Research Society, Pittsburgh, 1988), Vol. 99, p. 221.
[7] L. Krusin-Elbaum, A. P. Malozemoff, Y. Yeshurun, D. C. Cronemeyer, and F. Holtzberg, Physica C **153-155**, 1469 (1988).
[8] Y. Yeshurun, A. P. Malozemoff, and A. Shaulov, Rev. Mod. Phys. **68**, 911 (1996).
[9] Y. J. Uemura, L. P. Le, G. M. Luke, B. J. Sternlieb, W. D. Wu, J. H. Brewer, T. M. Riseman, C. L. Seaman, M. B. Maple, M. Ishikawa, D. G. Hinks, J. D. Jorgensen, G. Saito, and H. Yamochi, Phys. Rev. Lett. **66**, 2665 (1991).
[10] D. Shoenberg, *Superconductivity* (Cambridge University Press, Cambridge, 1952).
[11] B. M. Smolyak, E. V. Postrkhin, and G. V. Ermakov, Semicond. Sci. Technol. **7**, 427 (1994).
[12] V. I. Fesenko, V. N. Gorbunov, and V. P. Smilga, Physica C **176**, 551 (1991).
[13] A. Keren, A. Kanigel, J. S. Lord, and A. Amato, Solid State Commun. **126**, 39 (2003).
[14] Y. J. Uemura, G. M. Luke, B. J. Sternlieb, J. H. Brewer, J. F. Carolan, W. N. Hardy, R. Kadono, J. R. Kempton, R. F. Kiefl, S. R. Kreitzman, P. Mulhern, T. M. Riseman, D. Ll. Williams, B. X. Yang, S. Uchida, H. Takagi, J. Gopalakrishnan, A. W. Sleight, M. A. Subramanian, C. L. Chien, M. Z. Cieplak, Gang Xiao, V. Y. Lee, B. W. Statt, C. E. Stronach, W. J. Kossler, and X. H. Yu, Phys. Rev. Lett. **62**, 2317 (1989).
[15] Y. J. Uemura, Solid State Commun. **126**, 23 (2003).
[16] E. Polturak, D. Cohen, and A. Brokman, Solid State Commun. **68**, 671 (1988).
[17] Y. Zuev, M. S. Kim, and T. R. Lernberger, e-print cond-mat/0410135.
[18] A. Keren and A. Kanigel, Phys. Rev. B **68**, 012507 (2003); S. Sanna, G. Allodi, G. Concas, A. D. Hillier, and R. DeRenzi, Phys. Rev. Lett. **93**, 207001 (2004).